

# Probabilistic Analysis of Local Liquefaction Potential Based on Spatial Variability of SPT Data

Ali Gholampour<sup>1</sup>, Javad Shahsavar<sup>2\*</sup> and Ali Johari<sup>3</sup>

<sup>1</sup>Assistant Professor, Apadana  
Institute of Higher Education,  
Shiraz, Iran.

<sup>2</sup>Graduate Student, Shiraz  
University of Technology, Iran.

<sup>3</sup>Associated Professor, Shiraz  
University of Technology, Iran.

**\*Corresponding Author:**

✉ [shahsavar@gmail.com](mailto:shahsavar@gmail.com)

**Received:** 05 November, 2020

**Accepted:** 25 January, 2021

**Published:** 30 January, 2021



## ABSTRACT

In this paper, the spatial distribution of liquefaction potential is estimated using in-situ data from the Standard Penetration Test (SPT). For this purpose, a case study of a liquefiable soil at the Azad University of Qeshm is selected in the numerical modeling. After conducting the site investigation and determining SPT results at four boreholes, two distinct modeling approaches are implemented to evaluate the Liquefaction Potential Index (LPI) at the considered site; In the first method, the conditional random field for SPT data is generated in a layer-by-layer strategy and then, the LPI is obtained using a SPT-based empirical relations at each elemental column. On the other hand, in the second method, the LPI is first determined at each borehole location and then, this parameter is adopted as a stochastic variable in the construction of surficial conditional random field. It can be concluded that both approaches are able to capture the varying severity levels of liquefaction at most locations across the area of study. However, the comparison shows that using the first approach results in a more fluctuated LPI results with almost the same extremum values.

**Keywords:** Liquefaction potential, SPT, Conditional random field, Probabilistic analysis

## Introduction

The soil liquefaction phenomenon is an issue of concern to earthquake geotechnical engineers in recent years. Liquefaction is called to a state of saturated granular media that loses its shear strength due to the increase in pore water pressure and, consequently, displacements. With the occurrence of this phenomenon, saturated sandy soils will lose their strength due to seismic loadings, and soil particles will flow. According to many case studies, soil liquefaction is one of the most important reasons for damages to lifelines, buildings, and infrastructures [1]. Liquefaction can cause large displacements in the ground, soil failures, reduction of bearing capacity, differential settlements in foundations, and sand boiling. This phenomenon has been observed in many earthquakes such as Alaska (1964), Niigata (1964), Loma Prieta (1989), Kobe (1995), Chi Chi (1999), and recently at Shonbeh Bushehr (2013). Manjil Roodbar had the largest consequence of liquefaction in 1990 in Iran [2].

Soils are known as engineering materials with the most spatial changes of texture and resistance. The spatial uncertainty of soil properties has led to an analysis of issues such as estimating the location of the liquefaction in a significant function of the statistics and possibilities. Moreover, the inherent uncertainties of the characteristics which affect liquefaction dictate that this problem is of a probabilistic nature rather than being deterministic. In this regard, probabilistic methods have long been used to model the geotechnical properties of soil [3]. Probabilistic analysis provides a means of evaluating the combined effects of uncertainties and offers a logical framework for choosing factors of safety that are appropriate for the degree of uncertainty and the consequences of failure [4]. For instance, Juang et al. [5] investigated the risk-based liquefaction potential evaluation using SPTs, which defines a boundary that separates liquefaction from the no-liquefaction occurrence. Johari et al. [6] presented an analytical approach to probabilistic modeling of liquefaction based on shear wave velocity. Rezania et al. [7] had research based on evolutionary

polynomial regression for determination of liquefaction potential of sands and also, Baise and Lenz [8] presented an alternate approach which uses geostatistical analysis to evaluate spatial correlation to interpolate across geologic units, therefore, providing an estimate of the spatial extent of liquefaction potential within geologic boundaries.

In this research, it is attempted to compare two methods for determining the spatial distribution of the occurrence of liquefaction at a case study. For this purpose, modeling of spatial variation of SPT records is conducted using the conditional simulation method. In the first method, which is termed the local soil property approach, the conditional random field for SPT data is generated in a layer-by-layer strategy and then, the LPI is obtained using an SPT-based empirical relation. In the second method, which is called the averaged index approach, the LPI is first determined at each borehole location and then, this parameter is adopted as a stochastic variable in the construction of the surficial conditional random field. Finally, the obtained results are compared to each other.

## Evaluation of liquefaction potential

### Standard penetration test

The SPT is a well-known soil exploration test that is widely used to determine the in-situ properties of soil. The test is especially suited for cohesionless soils as the correlation between the SPT value and many resistance parameters are now well established. The SPT is performed from the base of a borehole where a drop weight of certain mass and falling distance drives a standardized cone into the soil. The number of blows required for a certain penetration depth is being recorded [9]. Several corrections are applied to SPT blow counts in order to achieve a normalized value prior to use. As the test progresses, soil samples and groundwater information are also collected. A record is made of the number of blows required to drive each 150 mm (6-in) segment into the soil. This is done until 450 mm depth is achieved or otherwise penetration refusal. The blows recorded for the first 150 mm are usually discarded because of fall-in and contamination in the hole. The number of hammer blows required to drive the sampler for the last 300 mm (12-in) is an

indication of the relative density of the material and is generally referred to as the Standard Penetration Number or SPT blow count Value (N) [10].

### Procedure of SPT-based liquefaction prediction

The SPT is one of the most usual in-situ tests in order to determine the resistance against liquefaction. Parameters that cause an increase in the resistance against liquefaction are density, strain before the earthquake, over consolidation ratio, lateral earth pressure and also high SPT number. In 1985 studies have been taken by Seed and Idriss [11] for a clean Sand to measure the least ratio of cyclic strain, which is expected for the occurrence of liquefaction in clean sand with a given SPT. Having fine ingredients can influence SPT, therefore, it must be calculated in the evaluation of the resistance against liquefaction [12].

Youd and Idriss [13] developed the following equations with the assistance of Seed and Idriss [11] for correction of  $(N_1)_{60}$  to an equivalent clean sand value,  $(N_1)_{60,cs}$ :

$$(N_1)_{60,cs} = \alpha + \beta(N_1)_{60} \quad (1)$$

Where  $(N_1)_{60}$  is the corrected SPT blow count normalized to the effective overburden stress of 100 kPa and  $\alpha$  and  $\beta$  are coefficients determined from the following equations [14]:

$$\alpha = 0 \quad FC \leq 5\% \quad (2a)$$

$$\alpha = \exp[1.76 - (190/FC^2)] \quad 5 < FC < 35\% \quad (2b)$$

$$\alpha = 5.0 \quad FC \geq 35\% \quad (2c)$$

$$\beta = 1.0 \quad FC \leq 5\% \quad (3a)$$

$$\beta = [0.99 + (FC^{1.5}/1000)] \quad 5 < FC < 35\% \quad (3b)$$

$$\beta = 1.2 \quad FC \geq 35\% \quad (3c)$$

The Fines Content (FC) shown in Table 1 is intended to accommodate the effect of fines content. They are consistent with the three classes of soils ( $FC \leq 5\%$ ,  $5 < FC < 35\%$ ,  $FC \geq 35\%$ ) considered in the Seed and Idriss [11] liquefaction evaluation procedure.

**Table 1**  
Fines content indicator.

| Fines Content, FC (%) | Fines Content Indicator, FCI |
|-----------------------|------------------------------|
| $FC \leq 5$           | 1                            |
| $5 < FC < 35$         | 2                            |
| $FC \geq 35$          | 3                            |

Several methods have been proposed in the literature to predict the occurrence of liquefaction. Johari et al. [15] had research based on reliability assessment of

liquefaction potential using the jointly distributed random variables method and aslo Johari et al. [16] investigated the reliability analysis of static liquefaction

of loose sand using the random Finite Element Method (FEM). Hanna et al. [17] proposed a method for developing the liquefaction potential based on General Regression Neural Network model (GRNN) analysis of field liquefaction performance records. Recently, Johari et al. [18] proposed a comparative study in reliability analysis of liquefaction potential of layered soil. In many of these methods, the empirical correlations were established to predict the occurrence or non-occurrence of liquefaction at the site, by applying the field records and earthquake properties. The "simplified procedure" is the most widely used method for the investigation of the liquefaction potential of sandy soils. In this method, the earthquake-induced cyclic stress ratio, CSR, is initially determined and then the cyclic resistance ratio, CRR, is calculated for the estimation of liquefaction potential. The factor of safety against liquefaction triggering of the soil at a specific depth is then defined as:

$$FS = \frac{CRR_{7.5}}{CSR_{7.5}} \quad (4)$$

It is noted that throughout this paper the terms CSR and CRR are referred to the reference earthquake magnitude of 7.5. If the value of safety factor, calculated by Eq. (4), for a particular case is less than 1, the occurrence of liquefaction is predicted, and on the other hand, if  $FS > 1$  then it is considered as a non-liquefied case.

The CRR is calculated based on  $(N_1)_{60,cs}$ . In the following relation, the amount of CRR is calculated for an earthquake with a magnitude of 7.5:

$$CRR_{7.5} = -0.485 + 0.289 \left[ \frac{(N_1)_{60,cs}}{35} \right] + \frac{0.739}{[35 - (N_1)_{60,cs}]^{0.5}} \quad (5)$$

As the conventional liquefaction potential assessment profoundly relies on empirical correlations, the CSR was estimated using the general formulation of the simplified method. Since CRR is by definition, equal to the critical CSR, the following relation was implemented in this research:

$$CSR_{7.5} = \left( \frac{0.65 r_d \left( \frac{\sigma_v}{\sigma'_v} \right) \left( \frac{a_{max}}{g} \right)}{MSF} \right) \quad (6)$$

Where  $a_{max}$  is the peak horizontal ground surface acceleration,  $g$  is the acceleration due to gravity,  $\sigma_v$  is the total overburden stress at critical depth and  $\sigma'_v$  is the effective overburden stress at critical depth. The parameter  $r_d$  is the stress reduction factor that provides an approximate correction for flexibility of the soil profile. For a depth  $z$  of less than 23 m, the term  $r_d$  can be calculated using the following equations:

$$r_d = 1.0 - 0.00765z \quad \text{for } z \leq 9.15 \text{ m} \quad (7a)$$

$$r_d = 1.174 - 0.0267z \quad \text{for } 9.15 < z \leq 23 \text{ m} \quad (7b)$$

MSF is the magnitude scaling factor that accounts for the effect of earthquake magnitude,  $M_w$ ):

$$MSF = \left( \frac{10^{2.24}}{M_w^{2.56}} \right) = \left( \frac{M_w}{7.5} \right)^{-2.56} \quad (8)$$

Where  $w(z) = 10 - 0.5z$  ( $z$  = depth in meters) and  $d_z$  is the differential increment of depth. In this study the potential liquefaction categories proposed by Sonmez [19] was used, which defined  $F_L$  as:

$$F_L = 0 \quad FS \geq 1.2 \quad (9a)$$

$$F_L = 1 - FS \quad FS < 0.95 \quad (9b)$$

$$F_L = 2 \times 10^6 e^{18.427 FS} \quad 1.2 > FS > 0.95 \quad (9c)$$

In this study, a discretized form of the LPI given by Luna and Frost [20] was used for calculating the liquefaction potential on each borehole as follows:

$$LPI = \sum_{i=1}^{NL} w_i F_{Li} H_i \quad (10)$$

Where  $H_i$  is the thickness of the discrete layer and is determined by the SPT sampling frequency ( $H_i = 0.1$  m for this study); NL is the number of soil layers.

## Geostatistical modeling

In-situ tests, in particular, can provide a good characterization of soil properties at the location where tests are performed, but inevitable uncertainty remains at locations that are not examined. As a solution, geostatistical approaches are applied in geotechnical engineering for assessing the effect of uncertainties in geotechnical predictions and quantifying the spatial variability of soil properties. The main purpose of using the geostatistical technique is providing the best estimate of the soil properties between known data, especially when sampling covers a very scarce portion of the total volume of soil [21].

## Random field theory

Soil is considered to be materials whose properties are related to spatial coordinates. In other words, the properties of this material type vary from point to point. It is not possible to use the typical statistics and probability methods based on the autonomy of the sample space. The use of random field theory to achieve the values at different points of the problem is presented as a solution to deal with this uncertainty. The theory of random field can effectively describe the spatial variability of soil properties by the correlation function. In fact, this theory is a prediction method based on the available general information, predicting the desired attribute for different points. In this method, the simulated properties of soil in very near points have nearly the same values as well as the independent values of the soil.

Conditional simulation models are used to maintain the changes' texture and generate the real variation for the random variable. In the conditional simulation, the

generator algorithm must conclude the random variable's measured values in the sampling points. Conditional simulation techniques can be divided into direct methods and indirect methods. Indirect conditional simulation methods are used when the mean and variance of the random function are known and constant. In fact, this type of simulation is applied to the random function under static conditions of the second order. These methods are based on indirect simulation production that will be converted into a conditioned mode during phases. The direct simulation methods, such as sequential Gaussian simulation, are used when the average data is not constant. This type of simulation is applied to the random function under the inherent static assumption. The sequential Gaussian simulation method is considered as one of the best methods for producing the orientation of a multi-multivariate Gaussian field which was implemented in this study.

### Steps in the proposed method

In this study, a random field-based program was coded in MATLAB to discretize the domain into 87,500 elements in both methods. Then, in the averaged index approach, the safety factor was calculated in the centre of each element at the borehole location using empirical relations. Next, the LPI was determined for each borehole. By considering LPI as a stochastic parameter, the surficial random field was estimated. Finally, all the procedures were put into the Monte-Carlo simulation and repeat for 1000 times. The averaged results were presented as the final output. In the local soil property approach, the random field of SPT data were generated in a layer-by-layer sequence at every two meters. Then, the LPI determined for each elemental column in the model. These steps were repeated 1000 times in sense of Monte-Carlo Simulation. Again, the average LPI results were illustrated as the output of this approach. Flowcharts for the average index approach and the local soil properties approach are shown in Fig.1 and Fig.2, respectively.

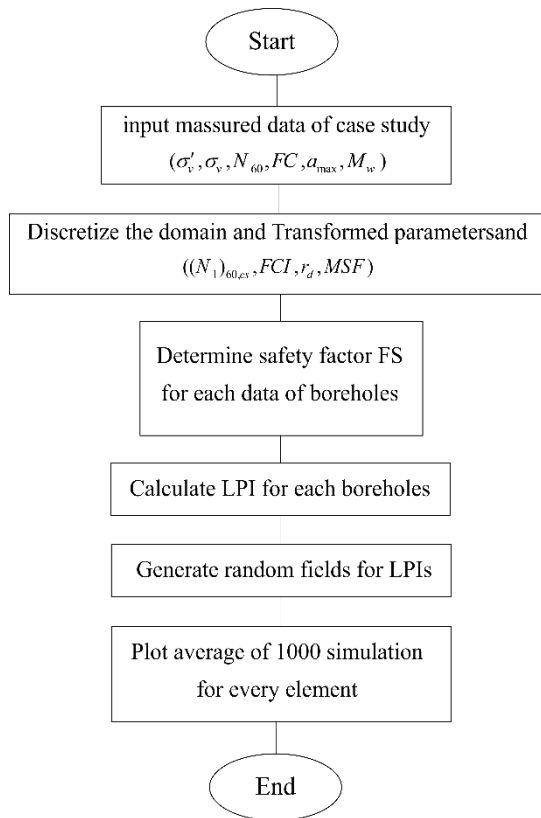


Figure 1. Flowchart of the averaged index approach.

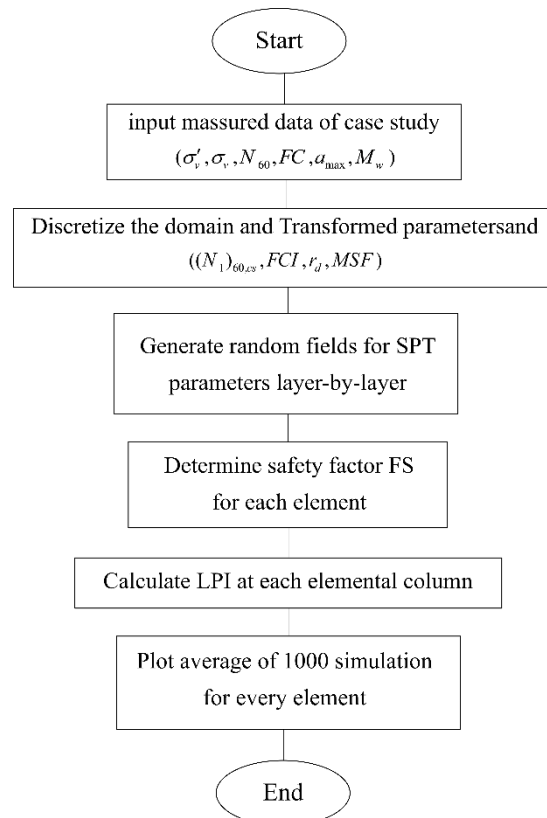


Figure 2. Flowchart of the local soil property approach.

### Case study

A case study of coarse-grained soil is selected for the evaluation of liquefaction potential. To probabilistically predict the liquefaction potential based on conditional random field, MATLAB-based programming was prepared. The whole dataset consists of 40 entries of SPT, bulk density and fine-grained content data that are the most important parameters for evaluating liquefaction potential.

### Site location and geotechnical soil properties

The site is on the Qeshm island of Iran, located in an urban area with an educational application. The site plan is shown in Fig.3. The main reason for selecting the site was that it mostly consists of coarse-grained soil located at a low-depth water table zone. In this situation, the liquefaction is the possible catastrophe for the soil systems under seismic load.

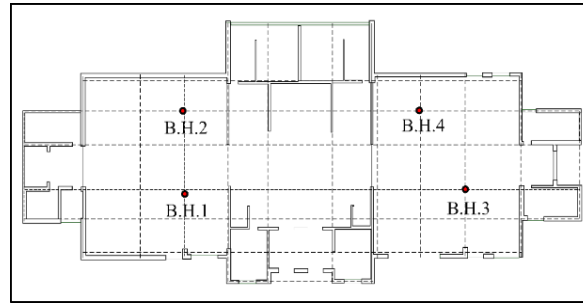


**Figure 3.** Plan of site and boreholes location.

To explore the subsurface layers, four boreholes were drilled to the depth of 20.0 m from the natural ground surface. As it is common in geotechnical projects, the boreholes are scattered distributed within the

considered area. For each borehole the field test (i.e., SPT) and laboratory tests (i.e., grain size analysis, Atterberg limits tests and so on) were performed. The borehole database is given in Tables 2 to 5.

**Table 2**

Soil properties from BH.1

| Depth | SPT | Bulk density (kg/cm <sup>3</sup> ) | Fine-grained content (%) |
|-------|-----|------------------------------------|--------------------------|
| 2     | 10  | 19.4                               | 30.47                    |
| 4     | 11  | 19.4                               | 60.22                    |
| 6     | 12  | 19.4                               | 97                       |
| 8     | 10  | 19.6                               | 98.8                     |
| 10    | 11  | 19.9                               | 88.4                     |
| 12    | 15  | 20.2                               | 61.71                    |
| 14    | 50  | 20.3                               | 76.05                    |
| 16    | 50  | 21.6                               | 76.32                    |
| 18    | 50  | 21.6                               | 51                       |
| 20    | 50  | 21.6                               | 79.56                    |

**Table 3**

Soil properties from BH.2

| Depth | SPT | Bulk density (kg/cm <sup>3</sup> ) | Fine-grained content (%) |
|-------|-----|------------------------------------|--------------------------|
| 2     | 5   | 19.3                               | 95.72                    |
| 4     | 7   | 19.4                               | 31.47                    |
| 6     | 5   | 19.5                               | 99.55                    |
| 8     | 6   | 19.4                               | 99.37                    |
| 10    | 11  | 19.4                               | 87.67                    |
| 12    | 11  | 19.9                               | 93.23                    |
| 14    | 28  | 20                                 | 95.9                     |
| 16    | 38  | 19.3                               | 99.4                     |
| 18    | 50  | 19.3                               | 99.25                    |
| 20    | 50  | 19.3                               | 95.55                    |

**Table 4**

Soil properties from BH.3

| Depth | SPT | Bulk density (kg/cm <sup>3</sup> ) | Fine-grained content (%) |
|-------|-----|------------------------------------|--------------------------|
| 2     | 8   | 19                                 | 57.51                    |
| 4     | 4   | 19                                 | 98.49                    |
| 6     | 3   | 19                                 | 94.96                    |
| 8     | 3   | 19.3                               | 97.53                    |
| 10    | 2   | 19.5                               | 99.46                    |
| 12    | 5   | 19.5                               | 76.02                    |
| 14    | 18  | 20.1                               | 71.67                    |
| 16    | 22  | 20.1                               | 71.96                    |
| 18    | 35  | 21.1                               | 69.43                    |
| 20    | 45  | 21.1                               | 54.3                     |

**Table 5**

Soil properties from BH.4

| Depth | SPT | Bulk density (kg/cm <sup>3</sup> ) | Fine-grained content (%) |
|-------|-----|------------------------------------|--------------------------|
| 2     | 15  | 19.9                               | 13.37                    |
| 4     | 13  | 19.9                               | 39.25                    |
| 6     | 7   | 19.5                               | 92.2                     |
| 8     | 5   | 19.9                               | 77.59                    |
| 10    | 6   | 19.4                               | 83.23                    |
| 12    | 9   | 19.5                               | 91.01                    |
| 14    | 11  | 19                                 | 59.57                    |
| 16    | 22  | 19.5                               | 96.65                    |
| 18    | 35  | 19                                 | 99.45                    |
| 20    | 45  | 19.5                               | 95.55                    |

## Results and discussions

As a way to interpret the calculated probability of liquefaction, five classes of liquefaction potential are defined, as shown in Table 6. These definitions of liquefaction potential classes are suitable for describing the likelihood of the occurrence of liquefaction.

Interpretation of liquefaction potential by means of the factor of safety is not as simple as that by means of the probability of liquefaction because the relation between the likelihood of liquefaction and the factor of safety is nonlinear. Thus, the interpretation of the calculated safety factor could be misleading if the concept or experience is extended to a different method [22].

**Table 6**

Liquefaction potential index classification.

| Liquefaction potential index (LPI) | Liquefaction potential classification |
|------------------------------------|---------------------------------------|
| 0                                  | Non-liquefiable                       |
| $0 < \text{LPI} \leq 2$            | Low                                   |
| $0 < \text{LPI} \leq 2$            | Moderate                              |
| $0 < \text{LPI} \leq 2$            | High                                  |
| $\text{LPI} > 15$                  | Very High                             |

At first, the average index approach was applied in the case study. Fig.4 shows the random field for one simulation of the calculated LPIs at four boreholes, using the average index approach. As shown in Fig. 4, most of the LPI at the BH.4 are greater than 20, and at BH.1 and BH.3, most of the LPIs simulated by this approach fall between 0 and 10, resulting in a sharp change in this range.

In the second step of analyzing, the local soil properties approach was implemented. In this method, random field simulations are performed for each soil layer with a thickness of 0.2 m. Fig. 5 shows the average of SPT fields for one soil layer at 16 m below the ground surface. The entire model of average SPT fields across the site for all soil layers is also shown in Fig.6.

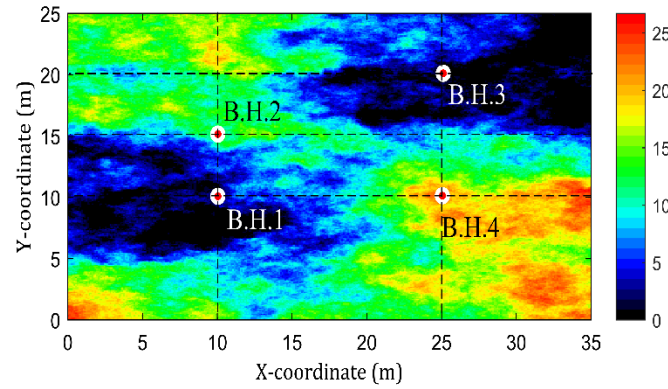


**Figure 4.** A conditional random field of one simulation for LPI parameters.

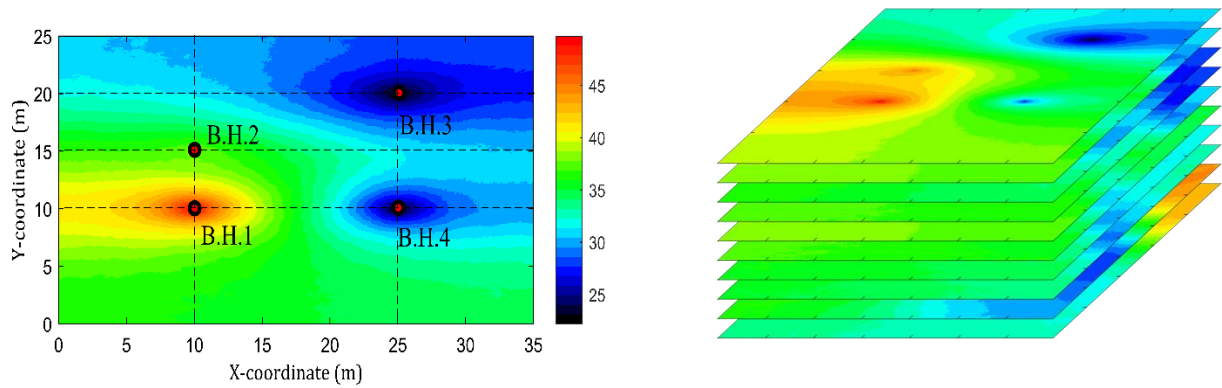


**Figure 5.** The average of SPT fields for one layer at a depth of 16 m.

**Figure 6.** The entire model of average SPT fields for all soil layers.

The generated LPI maps by average index and local soil properties approaches are illustrated as shown in Fig.7 and 8, respectively. It can be seen that both approaches are able to capture the varying severity levels of liquefaction at most locations across the area of study.

For instance, in both LPI fields, the high-value area which represents the very high liquefaction potential, corresponds well together. However, the results of the local soil property approach show more fluctuations.

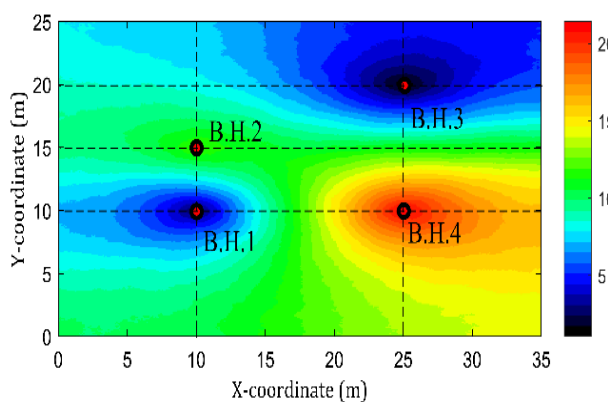


**Figure 7.** The average LPI from the averaged index approach across the studied site.

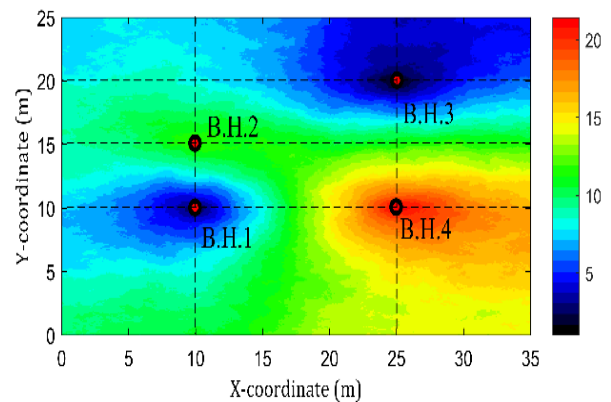


**Figure 8.** The average LPI from local property approach across the studied site.

## Conclusion

In this paper, a classical SPT-based empirical liquefaction model and the conditional random field techniques are integrated to assess regional liquefaction susceptibility. The study focuses on the spatial variability of SPT-based geotechnical parameters. Two approaches termed the averaged index approach and the local soil property approach, are analyzed to account for spatial variability of geotechnical parameters. Their implications on liquefaction susceptibility evaluation are discussed through one case study at the Azad University site in Qeshm island. It is concluded that the methods can identify the possible liquefaction location in which the area is determined based on the data contained in the borehole and the probabilistic analysis.

## References

1. Kasebzadeh J, Noorzad A, Mahboubi A, Manafi, M. Evaluation of liquefaction triggering considering the pertinent uncertainties. *Int Conf Civ Eng Archit Urban Sustain Dev*. 2013; Tabriz, Iran.
2. Kasebzadeh J, Noorzad, A. Liquefaction potential reduction near existing lifelines and residential buildings. *Sec Natl Conf Disast Manag Lifelin Minist Inter*. 2013; Tehran, Iran.
3. Shahsavari J, Gholampour A. Spatial probability distribution of liquefaction potential using conditional random field. *Int Conf Smart City*, 2019; Apadana Institute of Higher Education, Shiraz, Iran.
4. Johari A, Khodaparast AR. Modelling of probability liquefaction based on standard penetration tests using the jointly distributed random variables method. *Elsevier Eng Geol*. 2013; 158: 1-14.
5. Hsein Juang C, Caroline J. Chen, Tao Jiang, Ronald D. Andrus, Risk-based liquefaction potential evaluation using standard penetration tests. *Can Sci Publ J*. 2000; 37.
6. Johari A, Khodaparast AR, Javadi AA. An analytical approach to probabilistic modeling of liquefaction based on shear wave velocity. *Iran J Sci Tech Trans Civ Eng*. 2019; 43: 263-275.
7. Rezaei, Javadi, Giustolisi. Evaluation of liquefaction potential based on CPT results using evolutionary Polynomial regression. *Elsevier Comput Geotech*. 2010; 37: 82-92.
8. Jennifer A. Lenz, Laurie G. Baise. Spatial variability of liquefaction potential in regional mapping using CPT and SPT data. *Elsevier Soil Dynam Earthquake Eng*. 2007; 27(7): 690-702.
9. Md Manzur Rahman. Foundation design using

- standard penetration test (SPT) N-value. Bangladesh Water Development Board. 2020; <https://www.researchgate.net/publication/318110370>
10. Wazoh HN, Mallo SJ. Standard penetration test in engineering geological site investigations - A review. *Int J Eng Sci*. 2014; ISSN: 2319-1805.
  11. Seed HB, Idriss IM. Simplified procedure for evaluating soil liquefaction potential. *J Soil Mech Found Div*. 1985; ASCE 1971; 97(SM9): 1249-1273.
  12. Yousefzadeh Fard M, Babazadeh M, Yousefzadeh P. Soil liquefaction analysis based on geotechnical exploration and in situ test data in the Tabriz Metro Line 2. *Seven Int Conf Case Hist Geotech Eng*. 2013; Missouri University of Science and Technology.
  13. Youd TL, Idriss IM. Liquefaction resistance of soils: Summary report from the 1996 NCEER and 1998 NCEER/NSF workshops on evaluation of liquefaction resistance of soils. *J Geotech Geoenviron Eng*. 2001; ISSN: 1943-5606.
  14. Johari A, Khodaparast AR. Analytical reliability assessment of liquefaction potential based on cone penetration test results. *Sci Iranica Trans Civ Eng*. 2014; 21(5): 1549.
  15. Johari A, Javadi AA, Makiabadi MH, Khodaparast AR. Reliability assessment of liquefaction potential using the jointly distributed random variables method. *Elsevier Soil Dynam Earthquake Eng*. 2012; 38: 81-87.
  16. Johari A, Pour JR, Javadi A. Reliability analysis of static liquefaction of loose sand using the random finite element method. *Eng Comput*. 2015; 32(7).
  17. Hanna AM, Ural D, Saygili G. Neural network model for liquefaction potential in soil deposits using Turkey and Taiwan earthquake data. *Elsevier Soil Dynam Earthquake Eng*. 2007; 27: 521-540.
  18. Johari A, Rahnema H, Feilinejad A, Fotovat A. A comparative study in reliability analysis of liquefaction potential of layered soil. *Int Conf Civ Eng Architect Dev Reconstr Urban Infrastruct*. 2020; Tehran, Iran.
  19. Sonmez H. Modification of the liquefaction potential index and liquefaction susceptibility mapping for a liquefaction-prone area (Inegol, Turkey). *Int J Geosci Environ Geol*. 2003; 44(7): 862-871.
  20. Luna R, Frost JD. Spatial liquefaction analysis system. *J Comput Civ Eng*. 1998; 12(1): 48-56.
  21. Johari A, Gholampour A. A practical approach for reliability analysis of unsaturated slope by conditional random finite element method. *Elsevier Comput Geotech*. 2018; 102: 79-91.
  22. Wang C, Chen Q, Shen M, Juang CH. On the spatial variability of CPT-based geotechnical parameters for regional liquefaction evaluation. *Elsevier Soil Dynam Earthquake*, 2017; 153-166.



**SJIS**

**Copyright:** © 2021 The Author(s); This is an open-access article distributed under the terms of the Creative Commons Attribution License (<http://creativecommons.org/licenses/by/4.0>), which permits unrestricted use, distribution, and reproduction in any medium, provided the original work is properly cited.

**Citation:** Gholampour A, Shahsavar J, Johari A. Probabilistic Analysis of Local Liquefaction Potential Based on Spatial Variability of SPT Data. *SJIS*, 2021; 3(1): 21-29.

<https://doi.org/10.47176/sjis.3.1.21>